Bloch-Wave Analysis of Stripline- and Microstrip-Array Slow-Wave Structures

VITTORIO RIZZOLI, MEMBER, IEEE, AND ALESSANDRO LIPPARINI

Abstract—**The paper discusses a general approach to the analysis of periodic structures essentially consisting of an array of coupled striplines or microstrips. It is shown that any such structure can be represented as a cascade of identical multiport networks of known topology, thus allowing a straightforward analysis in terms of Bloch waves. The method is equally appitcable to homogeneous and nonhomogeneous dielectric (i.e., MIC) devices.**

I. Introduction

A GENERAL representation of the class of microstrip (or stripline) periodic slow-wave structures to be considered in this paper is schematically given in Fig. 1. The basic device consists of a uniform array of microstrips of finite length l that are suitably terminated at both ends of the coupled region. This is indicated in Fig. 1 by introducing the boundary networks Q_1, Q_2, which are assumed to be periodic with the same period d as the microstrip array, or a multiple thereof. The technical interest of this kind of device is well established, since a number of electrical functions can be realized by suitably specifying the topology of the boundary networks. This includes tight coupling (e.g., the combline directional coupler [1]–[2]), phase equalization (e.g., the meander line [3]–[5]), and filtering (e.g., the hairpin line [3]).

However, a unified treatment of these components from the standpoint of the classic theory of periodic structures has not been available so far. This is probably so because, while on one hand the network of Fig. 1 is clearly periodic, on the other the circuit topology of its fundamental cell is not immediately evident. In this paper we present and discuss a general method allowing periodic MIC devices to be analyzed and designed by a straightforward circuit approach. The basic mathematical tool for doing so is represented by Bloch waves.

II. Decomposition of a Microstrip-Array Device into a Cascade of Identical Cells

In this section we illustrate the transformation of the basic topology of Fig. 1 into a cascade of identical multiport networks (*fundamental cells*), which is a form suitable for Bloch-wave analysis. As shown in Fig. 1, a *unit cell* is defined as a section of the microstrip array bounded by the lengthwise centerlines of two adjacent strips. In the case that Q_1 and Q_2 are periodic with spatial period pd (p integer), the fundamental cell of the structure will consist of p cascaded unit cells of the array plus a section (corresponding to a period) of each boundary network. However, this basic configuration does not lend itself to a circuit analysis, since two consecutive cells are connected to each other along the entire centerline of a strip. Thus we must replace this distributed coupling by an equivalent set of discrete connections. This is made possible by the assumption of pure TEM (or quasi-TEM) propagation in the x-direction, as discussed below.

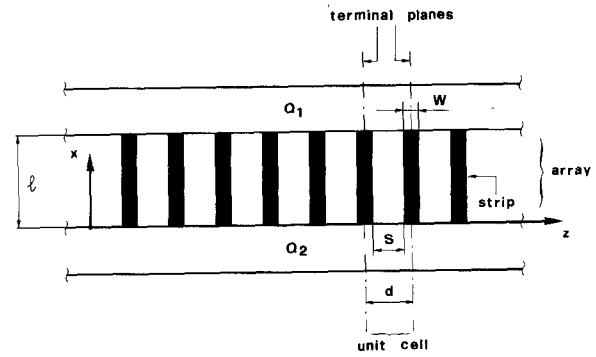

Fig. 1. General representation of a microstrip-array periodic structure.

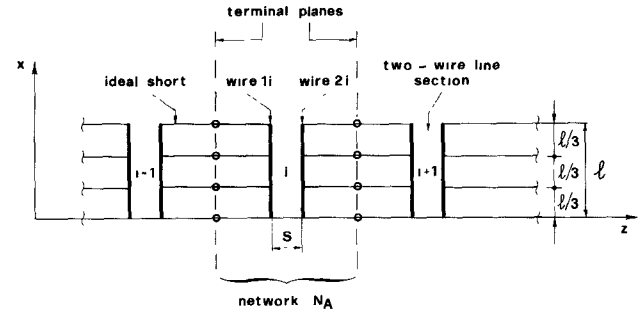

Fig. 2. Generation of a microstrip array by cascade connection of two-wire line sections.

As a preliminary step, we consider an infinite array of identical sections of symmetric two-wire lines uncoupled with each other (see Fig. 2). For the ith line the two conductors are indicated as wire 1 i and 2 i, and the amplitudes of the even- and odd-mode voltages traveling in the positive (negative) x-direction are denoted by V_{Ei}^{+}, V_{Oi}^{+} (V_{Ei}^{-}, V_{Oi}^{-}). Thus the voltages on wires 2 $i-1$ and 1 i

Manuscript received June 30, 1980; revised September 11, 1980.
The authors are with the Istituto di Elettronica, University of Bologna Villa Griffone, Pontecchio Marconi, Bologna, Italy.

0018-9480/81/0200-0143$00.75

may be expressed as

$$V_{2\,i-1}(x)=V_{Ei-1}^{+}\exp(-\gamma_E x)-V_{Oi-1}^{+}\exp(-\gamma_O x)+V_{Ei-1}^{-}\exp(\gamma_E x)-V_{Oi-1}^{-}\exp(\gamma_O x) \quad (1)$$

$$V_{1\,i}(x)=V_{Ei}^{+}\exp(-\gamma_E x)+V_{Oi}^{+}\exp(-\gamma_O x)+V_{Ei}^{-}\exp(\gamma_E x)+V_{Oi}^{-}\exp(\gamma_O x) \quad (2)$$

where γ_E, γ_O are the even- and odd-mode propagation constants. Now we establish short-circuit connections between the two wires considered at four different positions defined by

$$x_K=K\frac{l}{3}, \qquad K=0, 1, 2, 3 \quad (3)$$

as indicated in Fig. 2. This is mathematically equivalent to making $V_{2\,i-1}(x_K)=V_{1\,i}(x_K)$, or, from (1) and (2)

$$P_E^{+}\delta_E^{-K}+P_E^{-}\delta_E^{K}+P_O^{+}\delta_O^{-K}+P_O^{-}\delta_O^{K}=0, \qquad K=0, 1, 2, 3 \quad (4)$$

where

$$P_E^{+}=V_{Ei}^{+}-V_{Ei-1}^{+}$$
$$P_E^{-}=V_{Ei}^{-}-V_{Ei-1}^{-}$$
$$P_O^{+}=V_{Oi}^{+}+V_{Oi-1}^{+}$$
$$P_O^{-}=V_{Oi}^{-}+V_{Oi-1}^{-} \quad (5)$$

and

$$\delta_E=\exp\left(\frac{1}{3}\gamma_E l\right)$$
$$\delta_O=\exp\left(\frac{1}{3}\gamma_O l\right). \quad (6)$$

Equation (4) is a system of linear homogeneous equations in the unknowns (5), whose determinant is given by

$$\Delta=64\sinh\frac{\gamma_E l}{3}\cdot\sinh\frac{\gamma_O l}{3}\cdot\sinh^2\frac{(\gamma_E+\gamma_O)l}{6}\cdot\sinh^2\frac{(\gamma_E-\gamma_O)l}{6}. \quad (7)$$

Note that Δ is generally different from zero for $\gamma_E\neq\gamma_O$ (i.e., in the microstrip case). Thus the only solution of (4) is $P_E^{+}=P_E^{-}=P_O^{+}=P_O^{-}=0$. In turn, from (1), (2), and (5) we obtain

$$V_{2\,i-1}(x)=V_{1\,i}(x) \quad (8)$$

for any x.

In conclusion, making the connections indicated in Fig. 2 is equivalent to merging the wires $2\,i-1$ and $1\,i$ into a unique metal conductor. In this way, a uniform microstrip array such as shown in Fig. 1 can be generated from the set of isolated two-wire lines of Fig. 2. Fig. 3 illustrates the same concept in terms of capacitance models.

Conversely, given the device of Fig. 1, the microstrip array in it can be decomposed (as shown in Figs. 2 and 3) into a cascade of identical 8-port networks such as shown in Fig. 2 (network N_A in this figure), so that for the original periodic structure we find the equivalent circuit of Fig. 4. The topology of the fundamental cell is illustrated

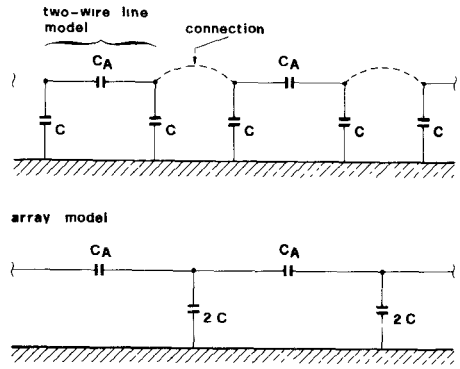

Fig. 3. Generation of a microstrip array from the standpoint of capacitance models.

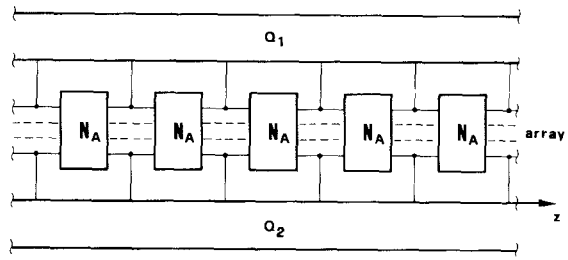

Fig. 4. General equivalent circuit of microstrip-array device.

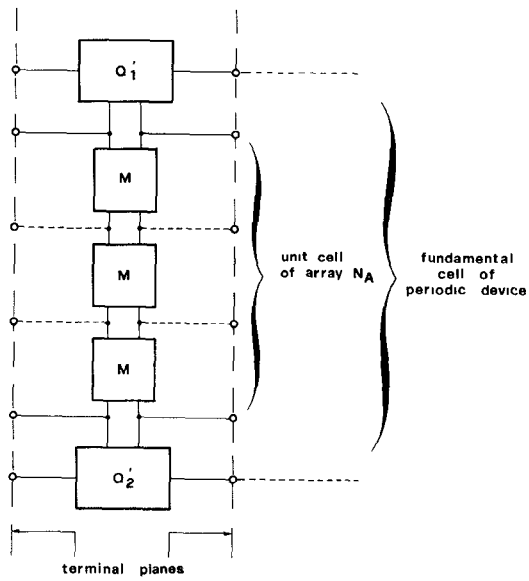

Fig. 5. Topology of the fundamental cell of a periodic device.

in some more detail in Fig. 5 for the case that Q_1 and Q_2 are periodic with the same period as the microstrip array. Here Q_1' and Q_2' are sections of Q_1 and Q_2 bounded by the terminal planes, while each block M represents a symmetric two-wire line of length $l/3$ (see Fig. 2). Such lines are defined by the capacitance model of Fig. 3(a), assuming that the capacitance model of the array is the one shown in Fig. 3(b).

In practical applications, one is given the geometrical parameters of the array (see Fig. 1), i.e., strip width (W), spacing (S), and length (l), as well as the topology of the boundary networks, and has to generate a circuit descrip-

tion (e.g., the scattering matrix) of the fundamental cell. According to the previous discussion, this can easily be accomplished by carrying out the following steps.

1) Starting from the geometrical data, the capacitance model of the array (Fig. 3(b)) is found by means of well-known static methods (e.g., the variational approach of [6]). The self and coupling capacitances are indicated by $2C$ and C_A, respectively, as in Fig. 3(b). The corresponding air capacitances (i.e., with the substrate dielectric constant set to one) are denoted by $2C'$ and C'_A.

2) The even- and odd-mode characteristic impedances and phase velocities of the two-wire line M (Fig. 5) are computed from the capacitance model of Fig. 3(a) by the following formulas:

$$Z_E = \frac{1}{v_0\sqrt{CC'}}$$

$$Z_O = \frac{1}{v_0\sqrt{(C+2C_A)(C'+2C'_A)}}$$

$$v_{pE} = v_0\sqrt{\frac{C'}{C}}$$

$$v_{pO} = v_0\sqrt{\frac{C'+2C'_A}{C+2C_A}} \tag{9}$$

where v_0 is the velocity of light *in vacuo*.

3) Making use of (9), the impedance (or admittance) matrix of the 4-port M is determined, e.g., by the explicit formulas reported in [7]. Then the networks Q'_1 and Q'_2 are analyzed (usually Q'_1, Q'_2 have very simple topologies and can be quantitatively described by conventional methods), and the various building blocks are combined [8] to find a circuit description—such as the scattering or transmission matrix—of the fundamental cell.

From the network of Fig. 4 all of the technically interesting particular cases can be simply generated by specifying the topologies of the boundary networks Q_1, Q_2. For instance, if Q_1 and Q_2 are cascades of transmission-line tees we get the combline coupler [1] (Fig. 6(a)), while for Q_1 and Q_2 reducing to transmission-line connections on alternate sides of the array, the microstrip meander-line is obtained (Fig. 6(b)). Note that for the above structures Q_1 and Q_2 are periodic with period $2d$ (i.e., twice that of the array), so that the fundamental cell of the periodic device contains two unit cells of the microstrip array. However the previously discussed guidelines for analyzing the fundamental cell are obviously still valid. Further circuit transformations may be sometimes carried out [9] in order to simplify the topology of the fundamental cell.

A final point concerns loss-free homogeneous-dielectric (i.e., ideal stripline) devices. In this case we have $\gamma_E = \gamma_O$, so that we are left with only two unknowns, namely, $P_E^+ + P_O^+$ and $P_E^- + P_O^-$, in the fundamental system (4). Thus the wires $2i-1$ and $1\ i$ need to be connected at only two locations (such as $x=0$ and $x=l$, see Fig. 2) to ensure the equality of the voltages at any value of x. As a consequence, the network N_A in the equivalent circuits of

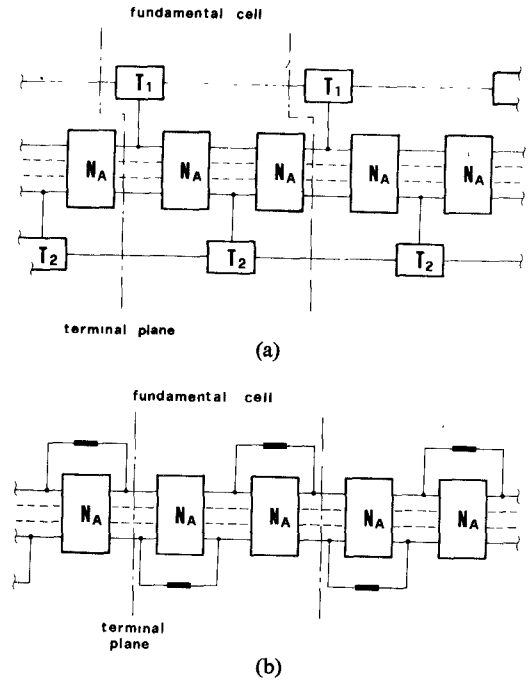

Fig. 6. Equivalent circuit of (a) the combline directional coupler, and (b) the microstrip meander line.

Figs. 4–6 will only have 4 ports (instead of 8), and the connections indicated by dashed lines in these figures will be missing. In particular, the three blocks M appearing in the fundamental cell (Fig. 5) will merge into a unique two-wire line of length l. All of the subsequent calculations will then be accordingly simplified.

III. General Analysis of a Microstrip-Array Periodic Structure

Any practical microstrip-array periodic device will consist of a cascade of identical fundamental cells terminated by suitable end sections. The latter may be separately analyzed and connected to the rest of the network by standard circuit algebra (e.g., [8]) once a circuit description of the cascade of repetitive cells has been found. The present section is devoted to the development of a Bloch-wave formalism for computing the scattering matrix of such a cascade.

According to [10], an electromagnetic field guided by the structure will be named a *Bloch wave* when the field distribution repeats identically at every terminal plane except for a propagation factor exp $(-\gamma)$. For general periodic structures, the Bloch-wave concept allows propagation along the device axis to be treated separately from the field description. The latter is thereby reduced to the analysis of a single fundamental cell, from which the dispersion equation for the Bloch waves supported by the structure is directly derived [10]. A general field may then be expressed by a superposition of Bloch waves, assuming that these represent a complete set of modes. This is conceptually similar to the usual treatment of uniform waveguides, where the mode concept allows the field analysis to be restricted to the waveguide cross section. For the present case, a *circuit* description of the funda-

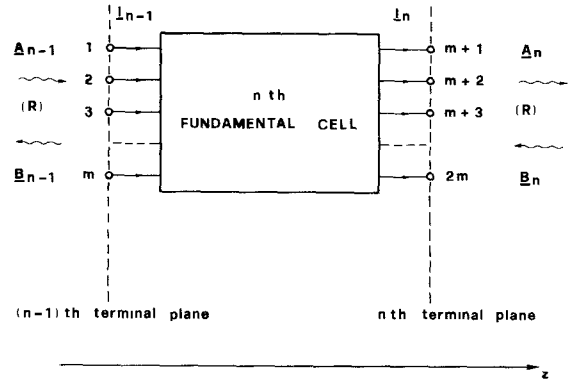

Fig. 7. Definition of forward- and backward-traveling wave amplitudes at the ports of the nth cell.

mental cell is available from the general discussion of Section II. In order to simplify the subsequent calculations, the incident and reflected wave amplitudes at the nth terminal plane, namely A_n, B_n, are used to describe the electrical behavior of the structure. These are related to voltages and currents by the usual relationships

$$A_n = \frac{1}{2}\left(\frac{1}{\sqrt{R_0}} V_n + \sqrt{R_0}\, I_n\right)$$

$$B_n = \frac{1}{2}\left(\frac{1}{\sqrt{R_0}} V_n - \sqrt{R_0}\, I_n\right) \tag{10}$$

(R_0 = reference impedance). Thus the equations of the fundamental cell take the form

$$\begin{bmatrix} A_{n-1} \\ B_{n-1} \end{bmatrix} = T \cdot \begin{bmatrix} A_n \\ B_n \end{bmatrix} \tag{11}$$

where T is the wave transmission matrix (see Fig. 7). Equation (11) can be viewed as a difference equation in the unknowns A_n, B_n, which for the present purposes replaces Maxwell's equations. Thus we can expect to be able to derive from (11) a dispersion equation for the Bloch waves supported by the structure. Obviously, since (11) is only valid under the assumption of quasi-TEM propagation in the x-direction, only Bloch waves undergoing this limitation will be obtained, in much the same way as only the quasi-TEM modes of an array of uniform coupled microstrips can be found starting from the classic coupled-line equations. These waves, however, can be expected to be the only significant ones for MIC applications.

Now let us denote by W_n a complete set of Bloch waves at the nth terminal plane. By definition of completeness, any electromagnetic field supported by the structure at the same plane—here described by the set of scalar quantities A_n, B_n—can be expressed as a linear combination of the elements of W_n, that is

$$\begin{bmatrix} A_n \\ B_n \end{bmatrix} = MW_n \tag{12}$$

where M is a square nonsingular matrix independent of n. Both the row size of M and W_n equals the number of ports of the fundamental cell, which is denoted by $2m$ (see Fig. 7). From (11) we get

$$W_{n-1} = \Lambda W_n \tag{13}$$

with

$$\Lambda = M^{-1} T M. \tag{14}$$

By definition, the elements of W_n are Bloch waves if Λ is a diagonal matrix. In this case (14) shows that the elements of Λ are the eigenvalues of T, while M is a matrix whose columns are linearly independent eigenvectors of T. If the ith nonzero element of Λ is expressed as

$$\lambda_i = \exp(\gamma_i) \qquad i = 1, 2, \cdots, 2m \tag{15}$$

γ_i has the physical meaning of normalized propagation constant of the ith wave. According to the definition of eigenvalues, (15) satisfy

$$\det\{T - \exp(\gamma) I\} = 0 \tag{16}$$

where γ stands for any of the γ_i's and I is the identity matrix of order $2m$. Equation (16) is the dispersion equation for the Bloch waves being considered.

In the commonly encountered case of a reciprocal device, we have

$$\Lambda = \begin{bmatrix} \Lambda_1 & 0 \\ 0 & \Lambda_1^{-1} \end{bmatrix} \tag{17}$$

so that only m independent Bloch waves (traveling in the positive and negative z-direction) are found. Thus if the eigenvector matrix is divided into square submatrices in the form

$$M = \begin{bmatrix} M_1 & M_2 \\ M_3 & M_4 \end{bmatrix} \tag{18}$$

the general solution to (11) has the expression

$$A_n = M_1 \Lambda_1^{-n} W_I + M_2 \Lambda_1^n W_R$$

$$B_n = M_3 \Lambda_1^{-n} W_I + M_4 \Lambda_1^n W_R \tag{19}$$

where W_I, W_R are vectors of incident and reflected Bloch waves at the input ($n=0$) plane.

Next we consider the cascade connection of any number N of fundamental cells, which may be regarded as a $2m$-port network. The scattering matrix of this network is indicated as

$$S_N = \begin{bmatrix} S_{N11} & S_{N12} \\ S_{N21} & S_{N22} \end{bmatrix} \tag{20}$$

where each submatrix is $m \times m$. All we need to find S_N is to write down (19) for $n=0$ and $n=N$ and to eliminate the vectors W_I, W_R between the two sets of equations obtained in this way. The results are

$$S_{N11} = (M_1 + M_2 R'_N)(M_3 + M_4 R'_N)^{-1}$$

$$S_{N21} = (M_4 \Lambda_1^N R'_N + M_3 \Lambda_1^{-N})(M_3 + M_4 R'_N)^{-1}$$

$$S_{N22} = (M_3 + M_4 R''_N)(M_1 + M_2 R''_N)^{-1} \tag{21}$$

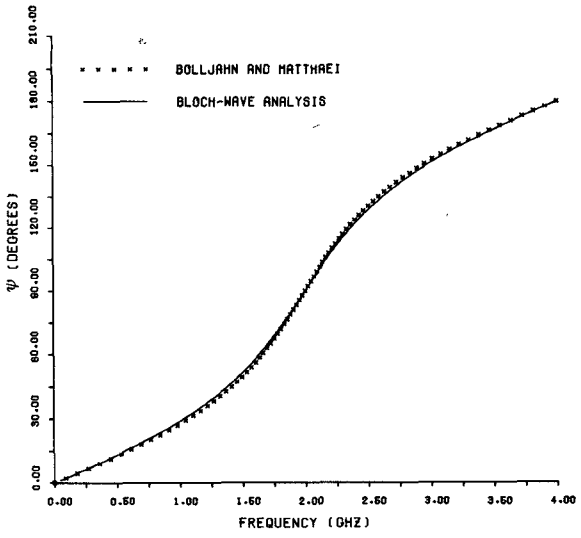

(a)

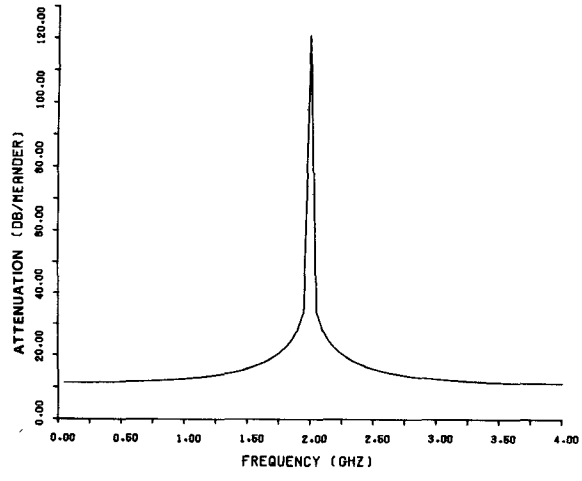

(b)

Fig. 8. Behavior of the two Bloch waves supported by a stripline meander equalizer. (a) Dispersion diagram of the propagating mode. (b) Attenuation constant of the cutoff mode.

where

$$\boldsymbol{R}'_N = -\Lambda_1^{-N}\boldsymbol{M}_2^{-1}\boldsymbol{M}_1\Lambda_1^N$$
$$\boldsymbol{R}''_N = -\Lambda_1^N\boldsymbol{M}_4^{-1}\boldsymbol{M}_3\Lambda_1^N. \tag{22}$$

Finally, by reciprocity

$$\boldsymbol{S}_{N\,12} = (\boldsymbol{S}_{N\,21})^T \tag{23}$$

with T denoting transposition. Thus starting from the knowledge of the wave transmission matrix the problem may be completely solved by elementary algebraic calculations.

An interesting point concerns the number m of independent Bloch waves supported by the structure. By inspection of Fig. 6 it is evident that m (which is half the number of ports of the fundamental cell) usually exceeds the number of propagating modes which can account for the electrical behavior of the device. For instance, a meander line with homogeneous dielectric is an all-pass network, whose performance resembles that of a conventional transmission line, except for the shape of the dispersion curve. This suggests single-mode operation, while a 4-port fundamental cell is found from Fig. 6(a). As a further example, a system of two coupled comblines in triplate configuration has an 8-port cell (Fig. 6(b)), but can be used to build codirectional couplers, which are typically two-mode devices. This is confirmed by experiments [1] showing the existence of only two propagating modes in such structures.

The above discrepancy is only apparent, since in most practical cases some of the Bloch waves obtained from (16) have a propagation constant with a large real part. These waves are strongly attenuated, so that they play a negligible role in the exchange of active power among the network ports. Thus the number of significant modes is considerably reduced. An example is given by the meander stripline defined by (25) below, for which two Bloch waves are found from (16). One of these has a purely imaginary propagation constant $\gamma = j\psi$, and its dispersion plot is given in Fig. 8(a) (solid curve); the other one undergoes an attenuation larger than 11 dB per meander at all frequencies (Fig. 8(b)), so that its effects are negligible for all practical purposes.

IV. Numerical Results

In this section we present and discuss a number of results concerning practical microstrip-array devices, that were obtained by the method previously outlined. A first point concerns the accuracy of the circuit equivalence described in Section II. It is easily found that the argument developed in that section leads to an analysis of the microstrip network which is only approximate. A rigorous analysis—still based on the quasi-TEM characterization of the array—would require the latter to be handled as a single circuit component consisting of a section of inhomogeneous ν-wire line, ν being the total number of strips. This would imply the existence of ν different phase velocities in the x-direction, while the present analysis only makes use of two. On the other hand, the memory storage and CPU time required by such an approach are quickly increasing functions of ν, while the use of the methods of Section III, and of (21) in particular, makes both storage and execution time *independent* of ν. Thus a design based on the rigorous approach can be extremely expensive in the case of a large device (such as, say, $\nu = 20$ or more).

As an example, we consider a microstrip meander-line equalizer with 19 meanders ($\nu = 20$), and assume that such a device has to be designed by computer optimization over a set of 7 frequency points. For this case the CPU time needed for each evaluation of the objective function via the direct method is found to be over 130 times as large as that required by the Bloch-wave approach. At current rates[1] a factor of over 130 usually means stepping from a moderately priced design to one that is not cost-effective. Closer examination shows that the Bloch-wave

[1]The cost of each function evaluation on a CDC Cyber 76 computer system was about $0.15 at the time of this writing (at the computing center CINECA, Casalecchio di Reno, Italy).

analysis actually makes use of the correct capacitance matrix of the array in the commonly encountered case of negligible capacitive couplings between nonadjacent strips. Thus the error is essentially confined to the evaluation of the inductive couplings.

Since a general error analysis would be difficult, the validity of the Bloch-wave approach was simply tested for a number of periodic devices with a limited number of cells. The exact quasi-TEM analysis was carried out by a general-purpose program for MIC design accepting arrays of up to 6 coupled microstrips as standard components [8]. In all cases the results were quite satisfactory. As a check, we present the data obtained for a microstrip 5-meander equalizer (i.e., 6 coupled strips) with the following parameters (see Fig. 1):

$$\begin{gathered}\text{substrate dielectric constant } \epsilon_r = 2.5 \\ \text{substrate thickness} = 1.575 \text{ mm} \\ \text{strip width } W = 4.36 \text{ mm} \\ \text{strip spacing } S = 0.194 \text{ mm} \\ \text{meander length } l = 27 \text{ mm}. \end{gathered} \tag{24}$$

Fig. 9(a) and (b) display a comparison between the exact quasi-TEM and the Bloch-wave analysis over a frequency range encompassing the first passband and the first stopband of the network. Note that the agreement is truly excellent for the phase delay (and thus for the group delay, too), which represents the key feature of the device operation. The good performance of the Bloch-wave approach is essentially due to the fact that the different phase velocities of the even and odd modes of the array are well averaged by the two velocities used in the periodic-structure analysis.

For a few simple structures with homogeneous dielectric, the results obtained from the Bloch-wave analysis may be directly compared with the classic explicit formulae given by Bolljahn and Matthaei [3]. For instance, let us consider a triplate meander line with the following geometry:

$$\begin{gathered}\text{dielectric constant } \epsilon_r = 2.5 \\ \text{ground plane spacing} = 3.15 \text{ mm} \\ \text{strip width } W = 2.06 \text{ mm} \\ \text{strip spacing } S = 0.2 \text{ mm} \\ \text{meander length } l = 23.7 \text{ mm}. \end{gathered} \tag{25}$$

According to [3], if further-than-nearest-neighbor capacitive couplings are neglected, the dispersion equation for this structure is

$$\cos\left(\omega\sqrt{\mu_0\epsilon_0\epsilon_r}\, l\right) = \frac{(1-2K_{12})\cos\psi}{1-K_{12}(1+\cos 2\psi)} \tag{26}$$

where ψ is the phase delay per meander and K_{12} is a coupling factor which is related to the capacitance model of the stripline array (Fig. 3(b)) by

$$\frac{1}{K_{12}} = \left[\sqrt{\frac{C}{2C_A}} + \sqrt{\frac{C}{2C_A}+1}\right]^2. \tag{27}$$

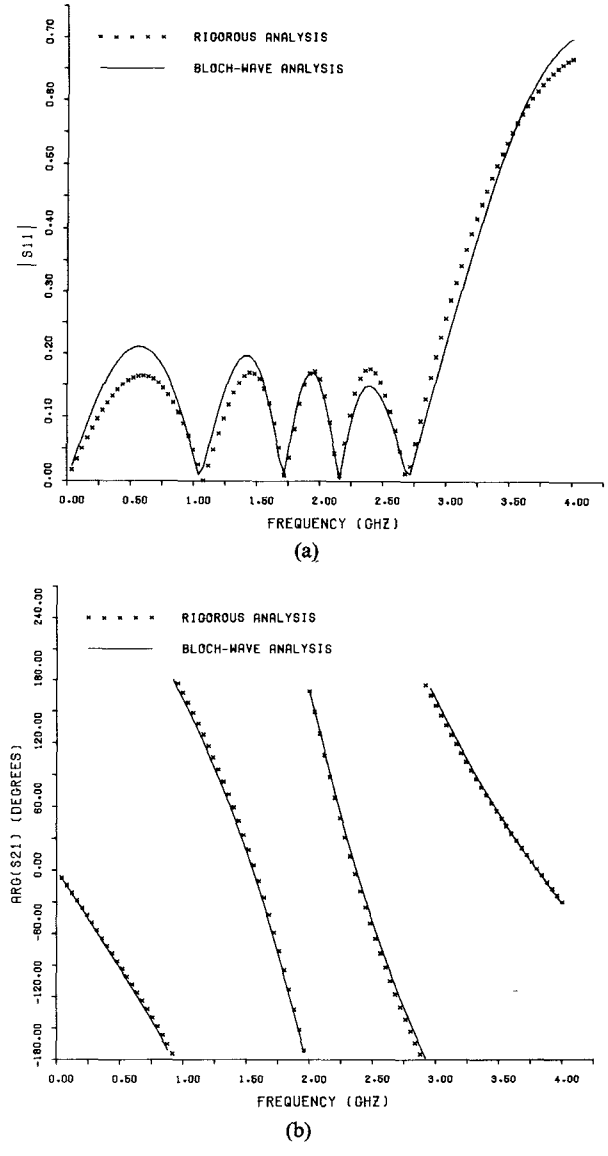

Fig. 9. Comparison of exact and Bloch-wave analysis of a microstrip meander line. (a) Magnitude of reflection coefficient. (b) Phase delay.

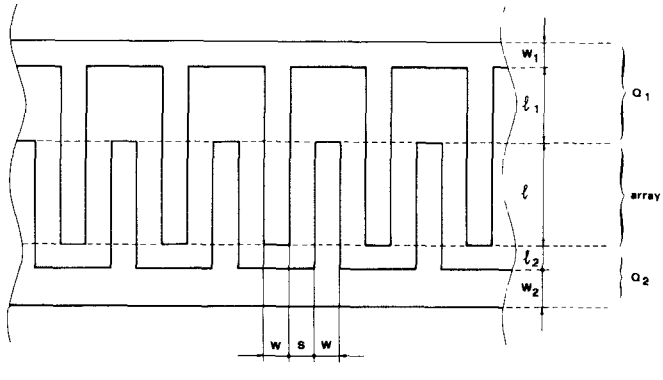

Fig. 10. Topology of a coupled-combline structure.

In this case the capacitance model is easily found by conformal mappings [6], yielding

$$K_{12} = 0.2707. \tag{28}$$

A plot of ψ versus frequency derived from (26) by means

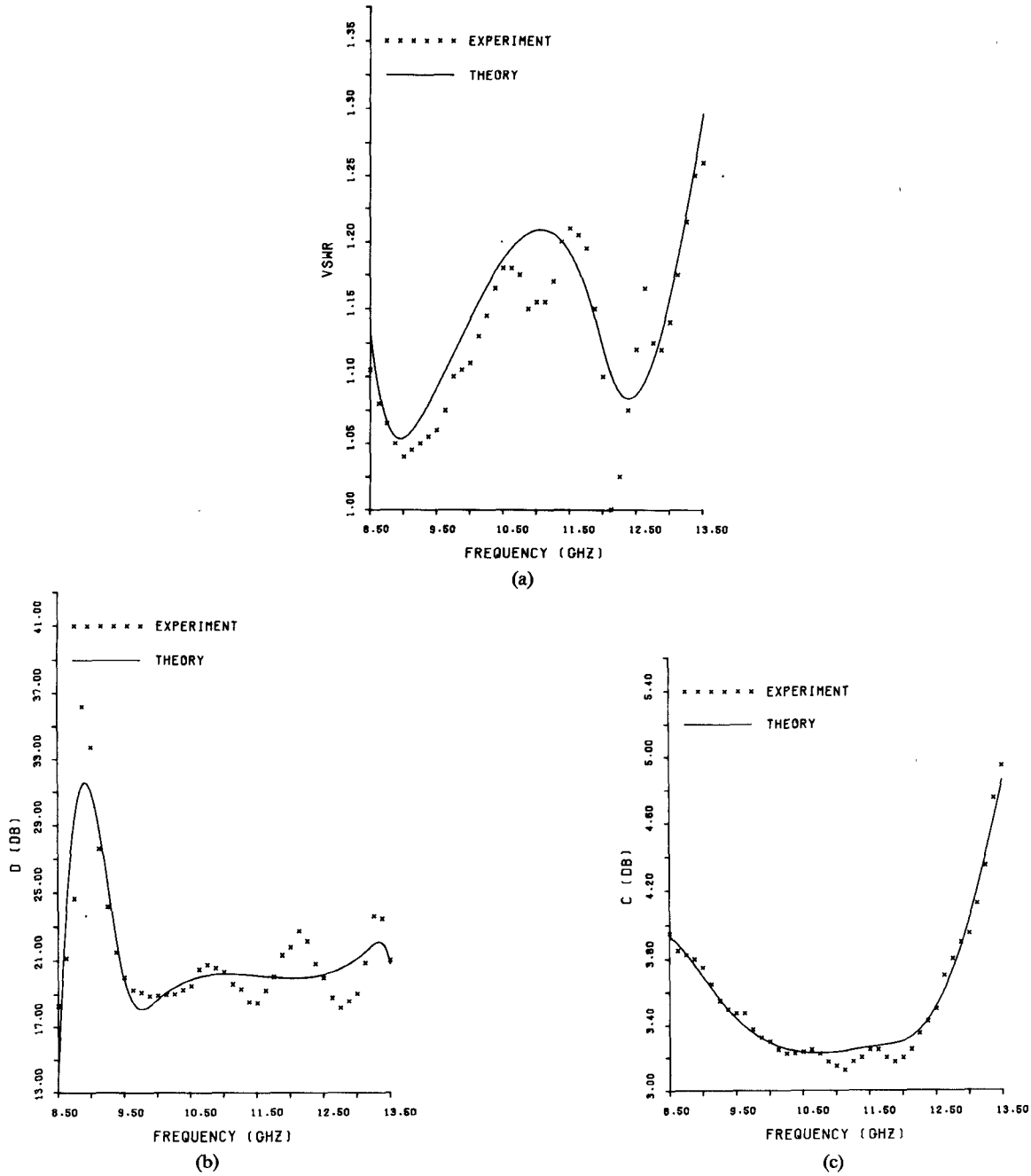

Fig. 11. Comparison between measured and computed performance of a combline directional coupler. (a) Input VSWR. (b) Directivity. (c) Coupling.

of (28) is given in Fig. 8(a) and is seen to match very closely the dispersion curve of the only propagating Bloch wave supported by the structure under consideration (see Section III).

Further confidence in the validity of the analysis approach described in this paper was gained by comparison of the computed and measured performance of periodic stripline and microstrip devices involving a large number of strips. A particularly significant example is given by the system of two coupled comblines illustrated in Fig. 10. This structure can be used for building planar codirectional couplers with tight coupling, both in stripline and microstrip configurations [1]. For instance, a stripline device made of an array of 25 coupled strips with the following geometrical parameters (see Fig. 10):

$$\begin{aligned} &\text{substrate dielectric constant } \epsilon_r = 2.32 \\ &\text{ground plane spacing} = 3.16 \text{ mm} \\ &W = S = 0.6 \text{ mm} \\ &W_1 = 0.92 \text{ mm} \\ &l_1 = 1.5 \text{ mm} \\ &l = 0.5 \text{ mm} \\ &l_2 = 0.3 \text{ mm} \\ &W_2 = 1.25 \text{ mm} \end{aligned} \tag{29}$$

will behave as a 3-dB coupler with about 30-percent bandwidth at 11 GHz, as reported by Gunton [1]. Fig. 11(a)–(c) show that the actual performance of the com-

bline coupler can be accurately predicted by the Bloch-wave analysis, in spite of its very complicated topology. To find the curves in Fig. 11 parasitic effects such as stray coupling capacitances at the strip open ends were accounted for by static methods. Minor discrepancies can probably be ascribed to the imperfect behavior of the terminations used to carry out the measurements [11]. The excellent accuracy of the Bloch-wave results shown in Fig. 11 is especially interesting in view of the fact that no alternative approach based on sound physical arguments is available to date for analyzing such devices.

References

[1] D. J. Gunton and E. G. S. Paige, "Directional coupler for gigahertz frequencies based on the coupling properties of two planar comb transmission lines," *Electron. Lett.*, vol. 11, pp. 406–408, 1975.

[2] D. J. Gunton, "Design of wideband codirectional couplers and their realization at microwave frequencies using coupled comblines," *IEE J. Microwaves, Opt., Acoust.*, vol. 2, pp. 19–30, 1978.

[3] J. T. Bolljahn and G. L. Matthaei, "A study of the phase and filter properties of arrays of parallel conductors between ground planes," *Proc. IRE*, vol. 50, pp. 299–311, 1962.

[4] R. Pregla, "Meander lines for delay equalization," in *Proc. Conf. Trunk Telecommunications by Guided Waves*, IEE Conf. Pub. N. 71, Sept. 1970, pp. 171–175.

[5] J. A. Weiss, "Dispersion and field analysis of a microstrip meander-line slow-wave structure," *IEEE Trans. Microwave Theory Tech.*, vol. MTT-22, pp. 1194–1201, Dec. 1974.

[6] J. I. Smith, "The even- and odd-mode capacitance parameters for coupled lines in suspended substrate," *IEEE Trans. Microwave Theory Tech.*, vol. MTT-19, pp. 424–431, May 1971.

[7] G. I. Zysman and A. K. Johnson, "Coupled transmission line networks in an inhomogeneous dielectric medium," *IEEE Trans. Microwave Theory Tech.*, vol. MTT-17, pp. 753–759, Oct. 1969.

[8] V. A. Monaco and P. Tiberio, "Computer-aided analysis of microwave circuits," *IEEE Trans. Microwave Theory Tech.*, vol. MTT-22, pp. 249–263, Mar. 1974.

[9] V. Rizzoli and A. Lipparini, "Coupled combline structures for use in M.I.C.'s," in *Proc. 8th European Microwave Conf.*, (Paris, France), Sept. 1978, pp. 84–88.

[10] R. E. Collin, *Foundation for Microwave Engineering*. New York: Mc-Graw Hill, 1966, pp. 369–390.

[11] V. Rizzoli and A. Lipparini, "A graphical approach to the design of multistrip components for M.I.C.'s," in *Proc. Int. Conf. Interactive Techniques in Computer-aided Design*, (Bologna, Italy), Sept. 1978, pp. 296–302.

Analysis of Small Aperture Coupling Between Rectangular Waveguide and Microstrip Line

J. S. RAO, K. K. JOSHI, AND B. N. DAS

Abstract—**This paper presents a generalized analysis on aperture coupling between a microstripline and a rectangular waveguide. The orthonormalized modal functions for the microstrip line required for the determination of the equivalent dipole moment are found from its equivalent parallel plate configuration. Expressions for coupling are obtained for transmission lines with their axes parallel, the lines forming a T-junction and also for cross-guide couplers. Theoretical results show good agreement with the experimental data for all cases under investigation.**

I. Introduction

IN ORDER to integrate waveguide circuitry with strip and microstrip circuitry, it is essential to realize coupling between these dissimilar lines. Some studies on the aperture coupling between a waveguide and a strip or a microstrip line with their axes parallel have been reported in the literature [1]–[4]. The coupling coefficient has been defined in the published literature as the ratio of the voltage in the coupled line to that in the primary line. The expressions obtained do not, however, exhibit reciprocal properties of the device.

In the present work the coupling between dissimilar guides is expressed as the ratio of the power flowing down the coupled guide to that in the primary guide. If the generator and coupled ports are designated as 1 and 2, respectively, the power coupling coefficients are the same for the directions 1→2 and 2→1. The expression for the power flow in a line is obtained from the product of the square of the model voltage [8] and the wave admittance of the propagating mode. For a TEM mode line the ratio of the modal voltage to modal current is equal to the wave admittance [7].

Analysis of aperture coupling between the rectangular waveguide and the microstrip line is restricted to small aperture, as the latter is replaced by its dipole moments [5], [6]. Amplitude of the modal voltage of the wave propagating in the coupled guide is determined from a knowledge of the equivalent dipole moment of the aperture and the orthonormalized field functions [8] in the coupled

Manuscript received June 9, 1980; revised September 30, 1980.

The authors are with the Department of Electronics and Electrical Communication Engineering, Indian Institute of Technology, Kharagpur-721302, India.

0018-9480/81/0200-0150$00.75 ©1981 IEEE